Design, Construction and Study of a new Gas Target for High-Order Harmonic Generation

Report by Tobias Eberle and Jan Klemmer

Lund Reports on Atomic Physics, LRAP-371
Lund, January 2007

Abstract

In this project a new gas target was constructed for high-order harmonic generation. It is characterised by a cell which length can be adjusted by adding small plates. To test this target we generated high-order harmonics of an intense infrared short pulse laser in Argon and measured the spectrum, angular divergence and intensity as a function of different parameters: pressure, focus position, IR pulse energy and diameter and target length. We also compare with the previous target which was a simple nozzle. We found that the intensity of the harmonics generated by the new target is roughly four times higher than by the old one. Furthermore the intensity is higher if the position of the focus is behind the medium and for larger target lengths. The harmonic' profile does not depend significantly on the focus position. Finally, we observe a shift from the long trajectory, selected by short target lengths, to the short trajectory, selected by long target lengths.

Contents

Chapter 1

Introduction

1.1 Background

Odd harmonics of the laser radiation are generated if a high intense short laser pulse interacts with atoms in a non-linear process. The intensity of these odd harmonics decrease exponentially with order before a long plateau is reached where the intensities of the harmonics are almost the same. After this plateau, in the cut-off region, the intensities decrease exponentially again and vanish completely. This effect, discovered experimentally in 1987, has been thoroughly explored. Nowadays many applications of higher-order harmonics are being developed: attosecond pulse generation, interferometry and holography, molecular orbital tomography, pump-probe spectroscopy, etc. One application recently explored in Lund is time-resolved digital holography which combines the short pulse duration of harmonics and their wavelength in the X-UV region to reach a time resolution to resolve biological or chemical processes on the one hand and a spatial resolution to do microscopy on the other hand.

1.2 Motivation

This project followed the master project "Towards Time-Resolved X-UV Digital in-line Holography" by Elena Mengotti and Guillaume Genoud ([3]). In that project X-UV radiation was used to perform time-resolved holography. The conclusion was that higher harmonic intensity was needed to do single shot holography. By building a new gas target, a cell with adjustable length, and optimising its intensity output by altering various phase matching parameters, we tried to address this problem. The parameters were pressure, focus position, pulse energy and aperture and target length.

1.3 Outline

In this report we start in Chapter 2 with a brief introduction of the theory of high-order harmonic generation. Instead of giving detailed derivations of formulas we focus on concepts and state only the most important formulas. Our experimental setup and the

new camera system for calibration is described in Chapter 3. Chapter 4 gives details about the design and construction of our new gas target. The experimental results are presented in Chapter 5 and discussed in Chapter 6. Finally, in Chapter 7 we draw some conclusions and give a short outlook. A detailed documentation of the setup can be found in Appendix A. This appendix can be used as future reference of how individual devices of the setup work or have to be used. Construction sketches of the new gas target can be found in Appendix B.

Chapter 2

Theory of high-order harmonics

In this section we briefly describe the process of high-order harmonics generation. This process can be observed when a strong electric field of a laser pulse interacts with atoms. In normal light propagation the emitted light from the medium has the same frequency as the incident light. Using an intense laser field, non-linear processes can take place and also odd multiples of the laser frequency can be observed. These processes occur when the electric field strength of the laser pulses is comparable to the inner-atomic fields.

Fig 2.1 shows a typical harmonic spectrum using argon.

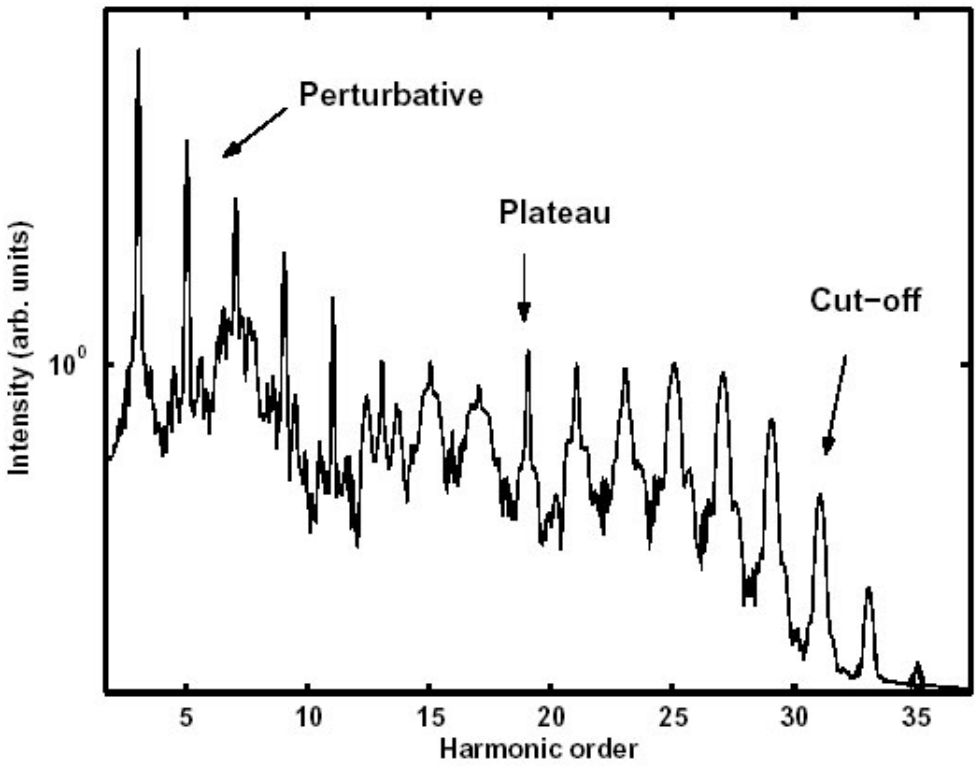

Figure 2.1: Typical harmonic spectrum using argon

The behaviour of the lowest harmonic orders are as one would expect from perturbation

theory: The intensity drops down with the harmonic order. It is followed by a plateau with almost constant intensity and an abrupt cut-off. This behaviour can be explained by the three-step model.

2.1 The three-step model

In this model it is assumed that an atom has only one electron. The electron motion is described partly classically. The steps are shown in Figure 2.2.

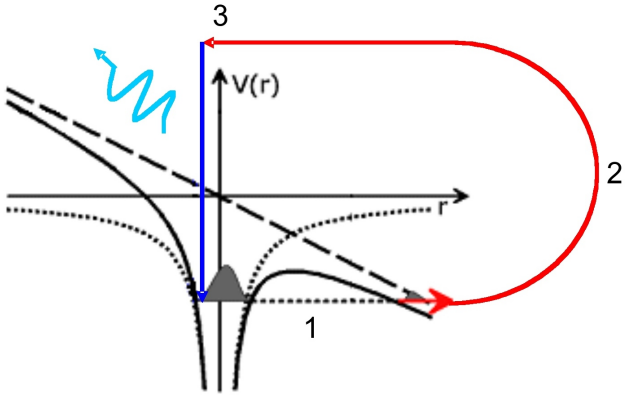

Figure 2.2: The three-step model for harmonics generation

1. When the electric field of the laser is near its maximum, the electron can tunnel through the distorted Coulomb barrier.

2. The electric field accelerates the electron away from the atom. When the electric field changes its sign the electron has the possibility to return to the ion core.

3. There is a certain probability that the electron recombines with the ion core. The gained energy is emitted as a photon.

This energy depends on the phase of the electric field at the time of emission and therefore on the excursion time while the electron is separated from the atom. Only for tunneling times $\frac{\pi}{2} < \omega t_i < \pi$ the electron can return to the ion core. The maximum kinetic energy the electron can gain is given by $3.2U_P$, where U_P is the ponderomotive energy. This is the average energy an electron can gain in an electric field and it can be calculated as

$$U_P = \frac{e^2 {E_0}^2}{4m\omega^2},$$

where e is the electron charge, E_0 the field strength, m the electron mass and ω the laser frequency. The maximum energy an emitted photon can have is

$$E = 3.2U_P + I_P,$$

where I_P is the ionisation potential of the atoms. This energy corresponds to the abrupt cut-off mentioned above. The ionisation potential influences the process of harmonics

generation: The higher it is, the higher is the harmonic order that can be obtained. We used Argon with an ionisation potential of 15.8 eV in our experiment.

The emission of photon energies up to the maximum energy has approximately the same probability. This leads to the plateau of peaks with nearly the same amplitude. The model also explains why we have peaks instead of a continuum and why there are only odd multiples of the driving frequency. The process of tunneling and recombination occurs twice per laser period T, so that the actual period time is $T/2$. Since the process is periodic in time it is also periodic in frequency with a periodicity of 2ω in the frequency domain. This is the reason why there are only odd harmonics.

For a more detailed description see [2].

2.2 Temporal description

Figure 2.3(a) shows the classical trajectories of the electric field corresponding to different tunneling times.

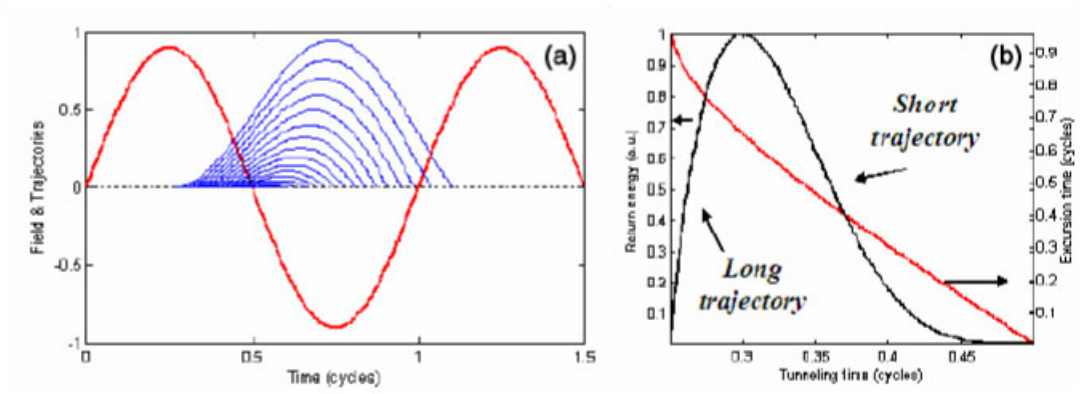

Figure 2.3: Temporal description of the harmonic generation process

One can see that the return energy is crucially dependent on the tunneling time. This can be seen better in Figure 2.3(b). Only tunneling times for which recombination is possible are shown. Every tunneling time corresponds to exactly one excursion time but there are two tunneling times corresponding to each return energy. These two different trajectories are called the long and the short trajectory and the emitted light has different properties for either of them.

2.3 Divergence of the long and the short trajectory

The phase the electron wave-packet gains in the continuum can be described by

$$\Phi \propto \alpha I(r,t),$$

where I is the intensity of the incident laser beam, r a spatial coordinate perpendicular to the propagation axis and α reflects the time spent by the electron in the continuum.

As an order of magnitude $\alpha = 20 \times 10^{-14}$ W^{-1}cm^2 for the long trajectory and $\alpha = 4 \times 10^{-14}$ W^{-1}cm^2 for the short one. With this phase we can write for the electric field of the harmonic:

$$E \propto e^{-i\Phi(r,t)} = e^{-i\alpha I(r,t)}.$$

The intensity I of the incident laser beam has a Gaussian profile rotationally symmetric around the propagation axis. The curvature of the wave front of the harmonic is therefore larger for larger α. Thus, the harmonic generated by the long trajectory which has a large curvature of the wave front, is more divergent as the one generated by the short trajectory with a smaller curvature of the wave front.

2.4 Gaussian beams

The laser field at the entrance of the nonlinear medium is usually taken to be a Gaussian beam. The electric field is then written as:

$$E(\mathbf{r}, t) = \frac{E_0 w_0}{w(z)} exp(-r^2/w^2(z)) exp(-i\omega t + i\Phi_G),$$

where E_0 is the field amplitude and Φ_G is the phase. The spot size radius, where the intensity has dropped to $1/e^2$ of the initial intensity is given by

$$w(z) = w_0\sqrt{1 + 4z^2/b^2}.$$

w_0 is the smallest spot size along the propagation axis and b is the confocal parameter:

$$b = \frac{2\pi {w_0}^2}{\lambda}.$$

The phase of the Gaussian beam is

$$\Phi_G = k_1 z - \Phi_f(z) + k_1 r^2/2R(z),$$

where

$$\Phi_f = \arctan(2z/b)$$

is the Gouy phase shift. $R(z)$ is the radius of curvature of the wave front:

$$R(z) = z + \frac{b^2}{4z}$$

2.5 Truncated Gaussian beams

We assume a Gaussian beam that passes an aperture where the wings are cut and is then focused by a lens. The beam after the lens ($z = z_0$) is then

$$E_0 = \tilde{E_0} e^{-{r_0}^2/w(z_0)^2} e^{ik{r_0}^2/2f}, r_0 \leq a$$

and

$$E_0 = 0, r_0 \geq a.$$

Here, r_0 is the coordinate transverse to the propagation direction at z_0, $\tilde{E_0}$ is the field amplitude, f is the focal length of the lens and a is the radius of the aperture. The field at the focal plane can then be calculated using the Huygens-Fresnel principle. Using cylindrical coordinates this field can be calculated as

$$E(r,z) = -ik_1 \int_0^\infty \frac{E_0(r_0,z_0)}{z-z_0} e^{\frac{ik_1}{2(z-z_0)}(r^2+{r_0}^2)} J_0(k_1 r r_0/(z-z_0)) r_0 dr_0,$$

where r_0 refers to the source coordinate, E_0 to the field at the position of the lens, J_0 is the zero order Bessel function.

Figure 2.4(a) shows an example for a truncated Gaussian beam. It is compared to Gaussian beams with different confocal parameters b. Figure 2.4(b) shows the corresponding phases.

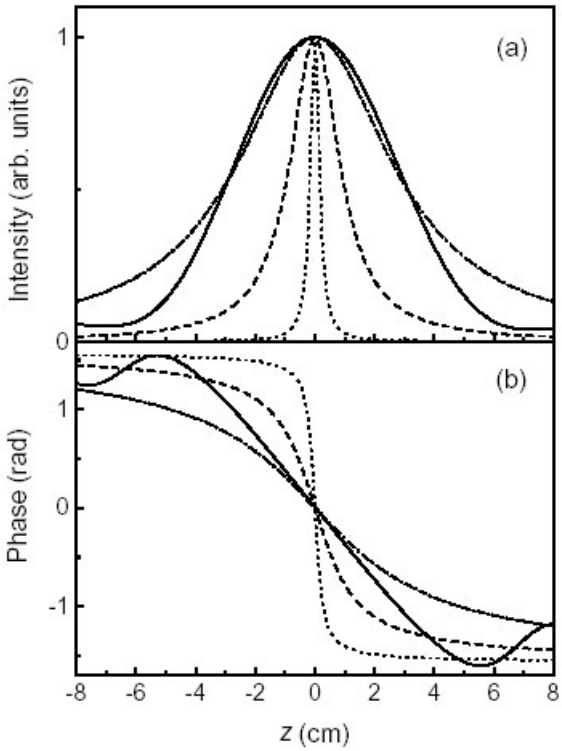

Figure 2.4: (a) Intensities of the truncated Gaussian beam with b=5 cm, truncated by a 2-cm aperture (solid line) and Gaussian beams with b = 3.3 mm (dotted line), b = 2 cm (dashed line), b = 6 cm (dot-dashed line). The focal length of the lens is f = 2 m. (b) The corresponding phases. [2]

The phase and the intensity of the truncated Gaussian beam changes much slower across the focus compared to the normal Gaussian beams. As seen before, the sum of the geometric phase and the dipole phase should vary as little as possible in order to minimize the phase mismatch. The dipole phase scales linearly with intensity. Therefore, the truncated Gaussian beam has an advantage compared to the normal Gaussian beam regarding phase matching.

2.6 Phase matching

An important aspect for the harmonic generation is phase matching. It basically means that the difference in wave vector between the incident laser beam and the generated harmonic must be minimized in order to get an efficient energy transfer between them. We consider a simple example to introduce the concept. According to perturbation theory ([2]) the laser field can be written as

$$E_1(z,t) = \frac{1}{2}[E_1(z)e^{i(k_1 z - \omega_0 t)} + c.c.].$$

If the second harmonic can be generated in the medium the non-linear polarization becomes

$$P_2{}^{NL} = \epsilon_0 \chi^{(2)} {E_1}^2 = \epsilon_0 \chi^{(2)} [{E_1}^2(z)e^{i(2k_1 z - 2\omega_0 t)} + c.c.].$$

The created electric field at frequency $2\omega_0$ is then

$$E_2(z,t) = \frac{1}{2}[E_2(z)e^{i(k_2 z - 2\omega_0 t)} + c.c.].$$

If we compare the polarization and the generated field we can see that they will propagate with different phase velocities if there is a mismatch in wave vector, i.e. $k_2 \neq 2k_1$. This is for instance the case if the medium shows dispersion and the refractive index depends on the frequency. The consequence of the different phase velocities is illustrated in Figure 2.5.

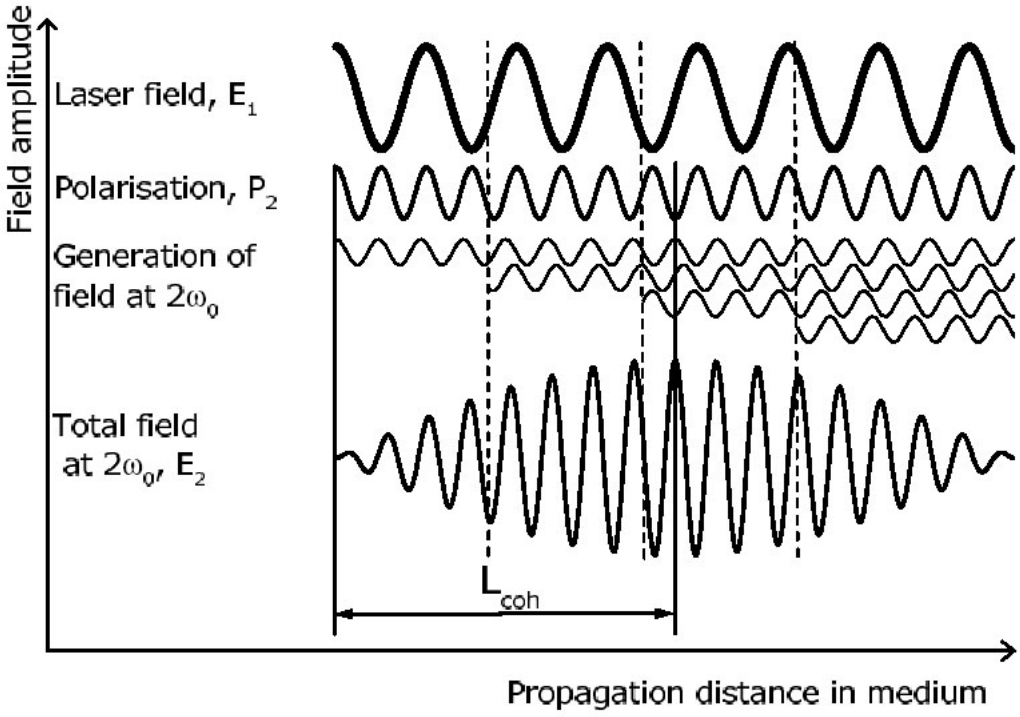

Figure 2.5: Consequences of the phase mismatch. The incident laser field and the induced polarization are shown at the top. Below one can see the generated wave-components at different positions of the medium. The bottom curve shows how these

components sum up to the total field coherently. This happens up to the coherence length. After this distance the field decreases due to the phase mismatch. [2]

The wavelets at frequency $2\omega_0$ generated by the polarization propagate with a different velocity than the laser field. Therefore the generated field at one point of the medium is not in phase with the field generated at another point. This results in a total field at frequency $2\omega_0$ that decreases after a certain distance in the medium. The distance where the field is built up constructively is called the coherence length L_{coh}. After this distance the polarization and the $2\omega_0$ wave have a phase difference of π, therefore

$$L_{coh} = \frac{\pi}{\Delta k}$$

with $\Delta k = k_2 - 2k_1$. The phase matching gets better the smaller Δk is.

2.6.1 On-Axis phase matching

For high-order harmonics generation more effects have to be taken into account. If we assume that the laser field is a Gaussian beam, the phase of the polarization on the propagation axis can be written as ([2])

$$\Phi_q{}^{pol} = \Phi_{dip} + qk_1 z - q \arctan(2z/b).$$

Here, q is the harmonic order. The dipole phase is is approximately given by

$$\Phi_{dip} = -\alpha I(z).$$

The laser wave vector depends on the refractive index: $k_1 = n_1\omega_0/c$. The term $\arctan(2z/b)$ is the Gouy phase shift, it shifts the phase by π across the focus.

In high-harmonic generation often only the geometric phase of the beam and the dipole phase have to be considered. Assume that the generated wave is a plane wave with wave vector $k_q = q\omega_0/c$ and the harmonic phase $\Phi_q = k_q z$. The phase difference between the generated harmonic and the polarisation is then

$$\delta\Phi_q = \Phi_q - \Phi_q{}^{pol} = \alpha I(z) + q \arctan\left(\frac{2z}{b}\right) + \Delta k_q z,$$

where Δk_q includes both the neutral atom dispersion and the influence of the free electrons. This phase difference has to be minimized in order to have a high conversion efficiency. Figure 2.6 shows an example for the phase difference.

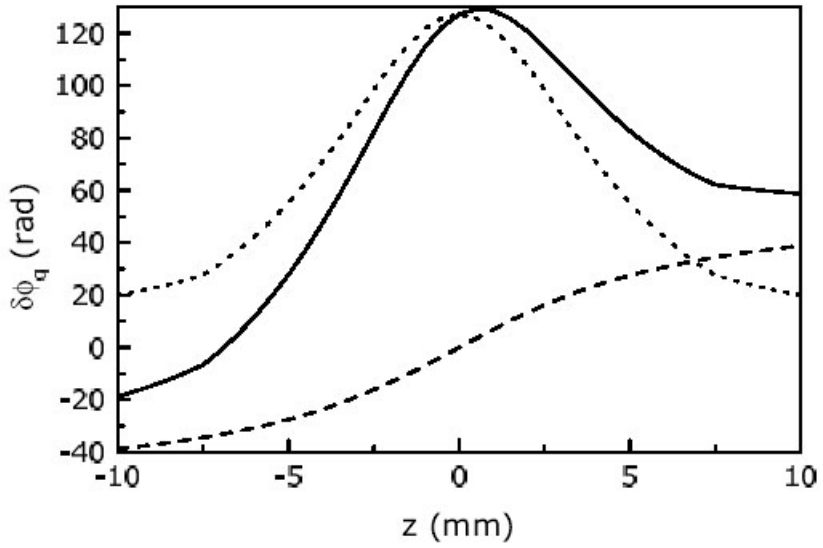

Figure 2.6: Example for the phase difference between the harmonic wave and the polarisation in Ne for the 35th harmonic. The confocal parameter is b=1 cm and the intensity $6 \cdot 10^{14} W/cm^2$. The dashed line is the geometrical phase shift of the Gaussian beam, the dotted line the dipole phase. The solid line shows the total phase difference. The focus is at $z = 0$, negative values mean positions before the focus. [2]

The focus is at $z = 0$. At about 7 mm after the focus, the geometrical and the dipole phase cancel each other out, so that the total phase difference is 0. In order to achieve on axis phase matching, the non-linear medium has to be placed at this position.

Chapter 3

Experimental setup

3.1 Setup

A sketch of the setup is shown in Figure 3.1.

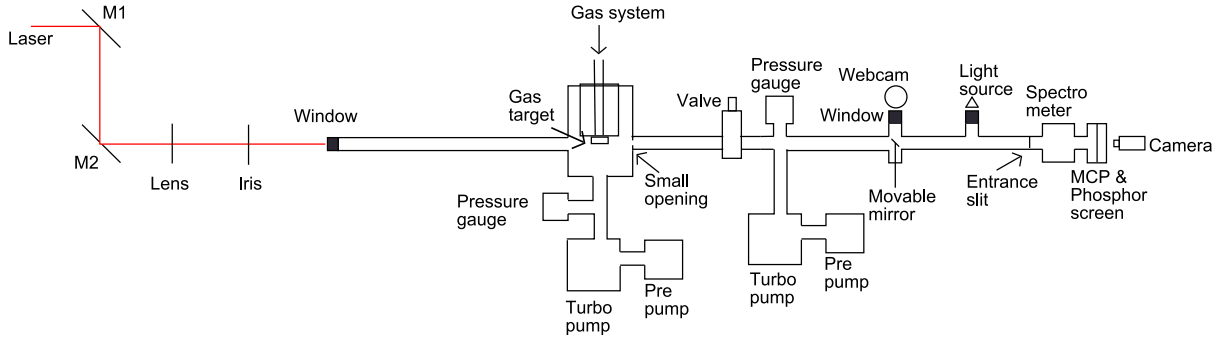

Figure 3.1: Experimental setup

Our experiment was carried out with the Terawatt laser at Lund High-Power Laser facility. It is a Ti:Saphire laser based on the chirped-pulse amplification technique. It has a repetition frequency of 10 Hz and a wavelength around 800 nm. We used pulses with a length of ca. 40 fs. A more detailed description of the laser system can be found in [3].

Mirrors $M1$ and $M2$ are used for the alignment of the beam. The lens has a focal length of 2 m and focuses the beam on the gas-target described in Chapter 4. The lens is mounted on a translation stage so that the position of the focus can be varied. The iris is used to reduce the beam power and for the alignment. The beam enters the vacuum system through a window. The pressure in the vacuum system was typically $10^{-5} - 10^{-6}$ mbar. Argon gas was used for harmonic generation. The small opening prevents that too much of the gas streams out of the target chamber.

The harmonics propagate collinear with the incident beam to the entrance slit of the spectrometer. The alignment could be controlled by using the movable mirror and the webcam which is described in the next section in more detail. A camera records the spectrum and the data can be acquired using a computer.

3.2 Camera system for calibration

One main improvement of the setup was to introduce a webcam to watch the entrance slit of the spectrometer in order to simplify the alignment. A sketch is shown in Figure 3.2.

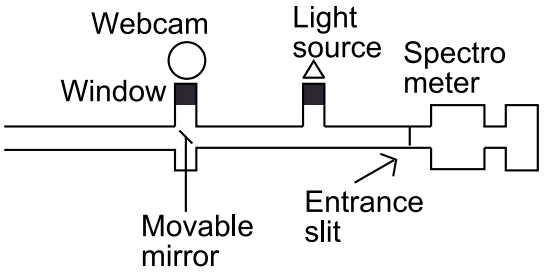

Figure 3.2: The camera system to control the alignment

If the mirror has the right position and angle, the entrance slit of the spectrometer can be observed using a webcam. The slit is illuminated by a light source. To avoid noisy pictures due to a lack of light a very bright lamp should be used, which was a standard desk lamp in our case. The webcam is sensitive in the infrared region, therefore it is possible to see if the laser beam hits the slit. Without this system it would be necessary to destroy the vacuum and to control the position of the laser 'by hand' every time the system has to be aligned. Since this has to be done very often it is a real improvement in effectivity.

3.3 Detection

In order to separate the harmonics with different wavelengths we used a spectrometer (I.S.A. Jobin-Yvon PGM PGS 200). The principle is shown in Figure 3.3.

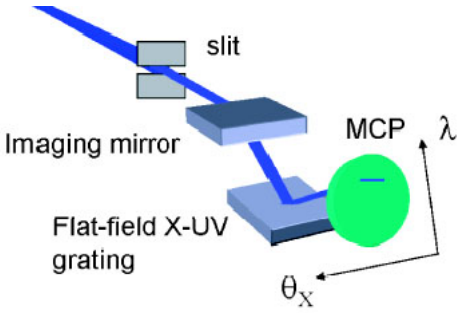

Figure 3.3: Principle of the spectrometer [3]

After the entrance slit the beam is focused by a toroidal mirror on a X-UV grating. The grating position can be varied so that different harmonic orders could be observed. The radiation leaves the spectrometer through an exit slit and is amplified by a microchannel plate (MCP), Figure 3.4.

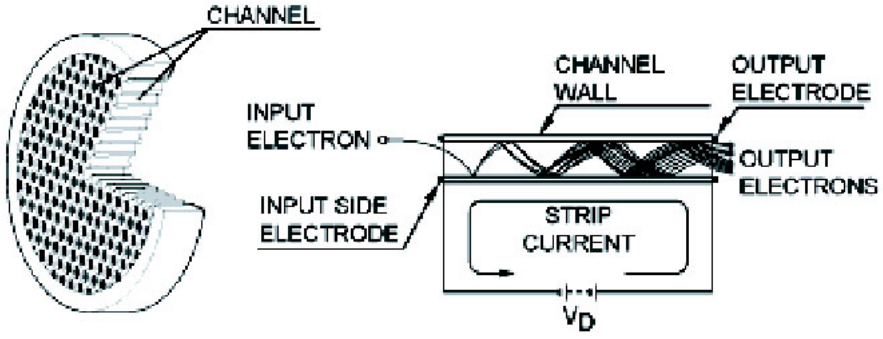

Figure 3.4: MCP and a straight channel electron multiplier

The MCP has a diameter of 60 mm and consists of an array of 104-107 miniature electron multipliers oriented parallel to each other. The channels have a typical diameter of 10-100 μm. When the X-UV photons hit the surface of the MCP, electrons are created. These electrons travel inside the channels and are accelerated by a strong electric field. They are scattered on the walls of the channel, producing more and more electrons. The signal is hereby amplified by several orders of magnitude and the electrons are made visible using a phosphor screen. For using the MCP the background pressure has to be $< 10^{-5}$ mbar.

Chapter 4

Design and construction of a new gas target

Our goal was to replace the existing gas target and try to increase the intensity of the created harmonics.

4.1 The old gas target

A sketch of the old target is shown in Figure 4.1.

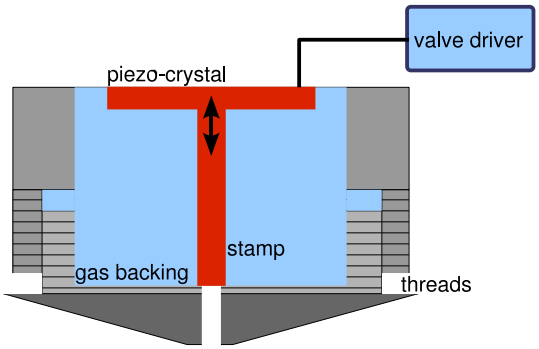

Figure 4.1: Sketch of the old gas target. The gas is released by a piezo mechanism.[4]

It is a valve filled with Argon gas. By applying a voltage on the piezo-crystal, the stamp is moved and the gas is released. The target for the harmonics generation is the gas jet that leaves the valve. The delay between the opening of the valve and the laser pulse is adjusted by a delay box so that there is a sufficient amount of gas in the chamber when the laser pulse arrives. The advantage of this trigger-mechanism is that the background pressure in the chamber is minimized. Since the trigger frequency of the laser is 10 Hz, the valve stays closed 99% of the time.

4.2 The new gas target

We invented a target that could be mounted on the existing system. In principle, the gas streams through a small tube where the laser beam is guided through. The gas is released by the same piezo mechanism as used for the old target. It enters our target through a hole on the bottom side, see Figure 4.2.

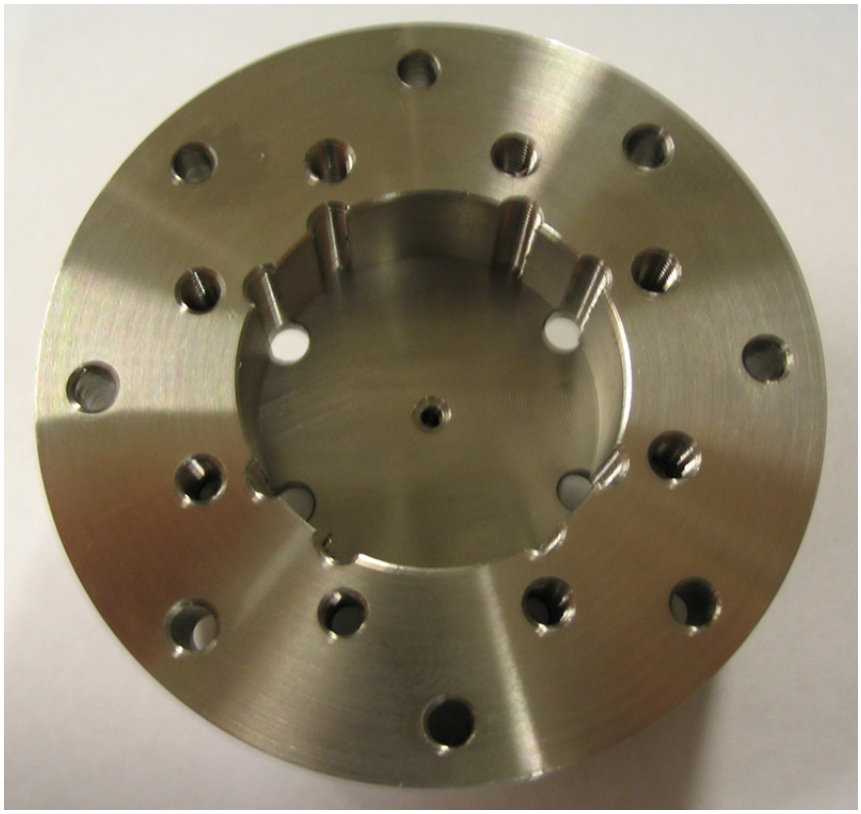

Figure 4.2: New Target, Bottom view. The gas enters through the hole in the middle

It streams through a tube where the laser beam is sent through. This tube can be seen in the middle of the four holes in Figure 4.3.

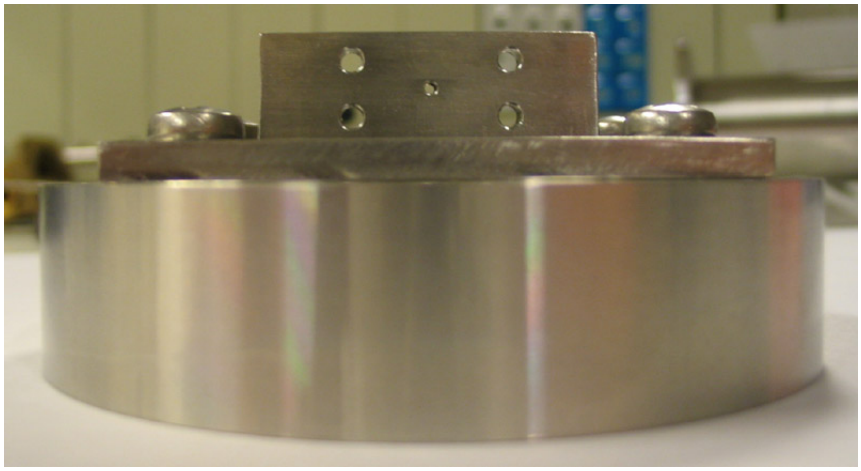

Figure 4.3: New Target, Side view. The gas streams through the hole in the middle

Figure 4.4 shows a top view of the target.

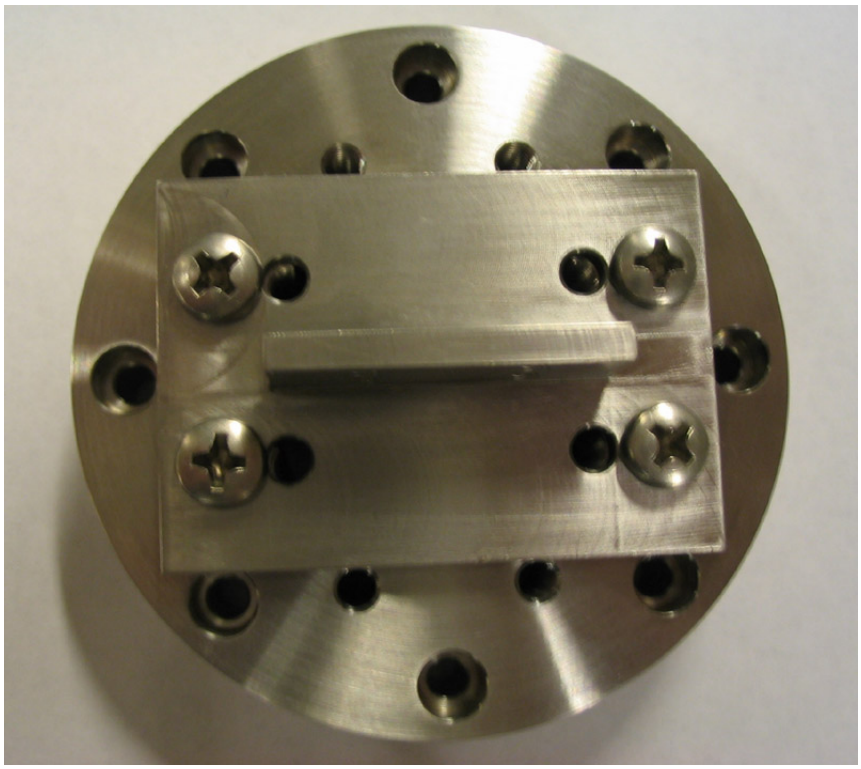

Figure 4.4: New Target, Bottom view. The gas enters through the hole in the middle

The tube has a length of 3 mm and a diameter of 1 mm. The complete drawings for the construction can be found in Appendix B.

The gas density in our target is much higher than it is in the gas jet of the old target. We wanted to study how this influences the intensity and shape of the harmonics. In addition, we were able to vary the length of the tube by adding plates on both sides of the target. Therefore it was possible to study the influence of the medium length on the process of harmonic generation. The plates are shown in Figure 4.5.

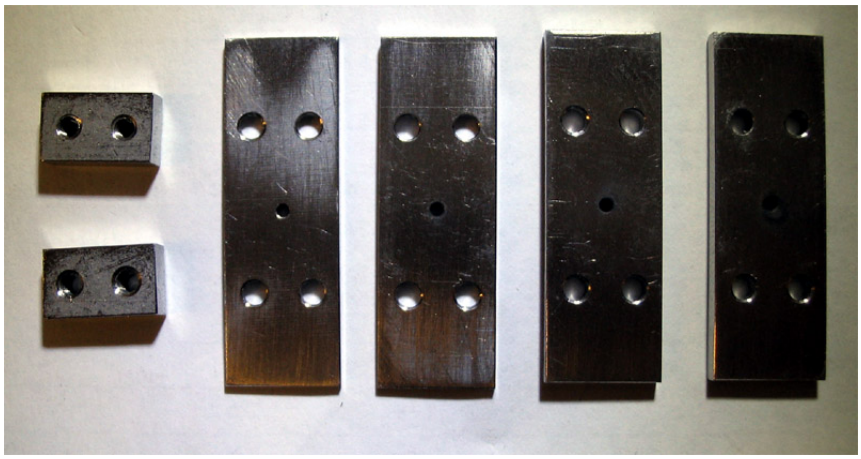

Figure 4.5: Plates for the elongation of our target.

We used two plates with a thickness of 1 mm and two plates with 2 mm. With these

plates it is possible to make measurements with tube lengths 3 mm, 5 mm, 7 mm and 9 mm. The two pieces on the left are used as endings for the screws.

Another interesting possibility would be to vary the tube length non symmetrical on both sides or to use plates where the hole has a diameter different than 1 mm. In these cases the pressure distribution in the tube might change and the process of harmonics generation would be influenced.

Chapter 5

Experimental Results

In this section we characterise the new gas target and compare it with the nozzle. First we look at the pressure dependence of the intensities of high-order harmonics for different focus positions. Then pressure and focus are fixed and aperture and energy of the beam are changed. After this we study the spatial distribution of the harmonics as a function of focus position and target length.

5.1 Calibration

To determine which harmonic in the spectra belongs to which order we plotted the pixel position of the maxima of the harmonics against their wavelength 800 nm/q, where q is a guessed harmonic order. This was done with different guesses of harmonic orders. For each plot a straight line was fitted and the one with a χ^2 closest to 1 was chosen. Following the described procedure we got orders from 19 to 27 for our five observed harmonics.

5.2 Pressure and Focus Position Dependence

For a pulse energy of 7 mJ and an aperture diameter of 8 mm we measured the pressure dependence of the intensity of the harmonics for different focus positions. In our notation a negative focus position means that the focus is in front of the middle of the medium and a positive one that it is behind. The pressure we are referring to is not the pressure in the target but the background pressure. The actual pressure in the cell is at least a factor of 10 less than the background pressure and not known.

Figure 5.1 shows the results for the 23rd harmonic for target lengths of 3, 5, 7 and 9 mm. Figure 5.2 shows the same for the 21st harmonic for the nozzle. The intensities are almost constant for the 3 mm target and for the other three target lengths they decrease a bit with increasing pressure. For the nozzle the intensities increase with pressure. This behaviour is independent of the focus position for all targets. The harmonic' intensities decrease with increasing target length. For different focus positions the

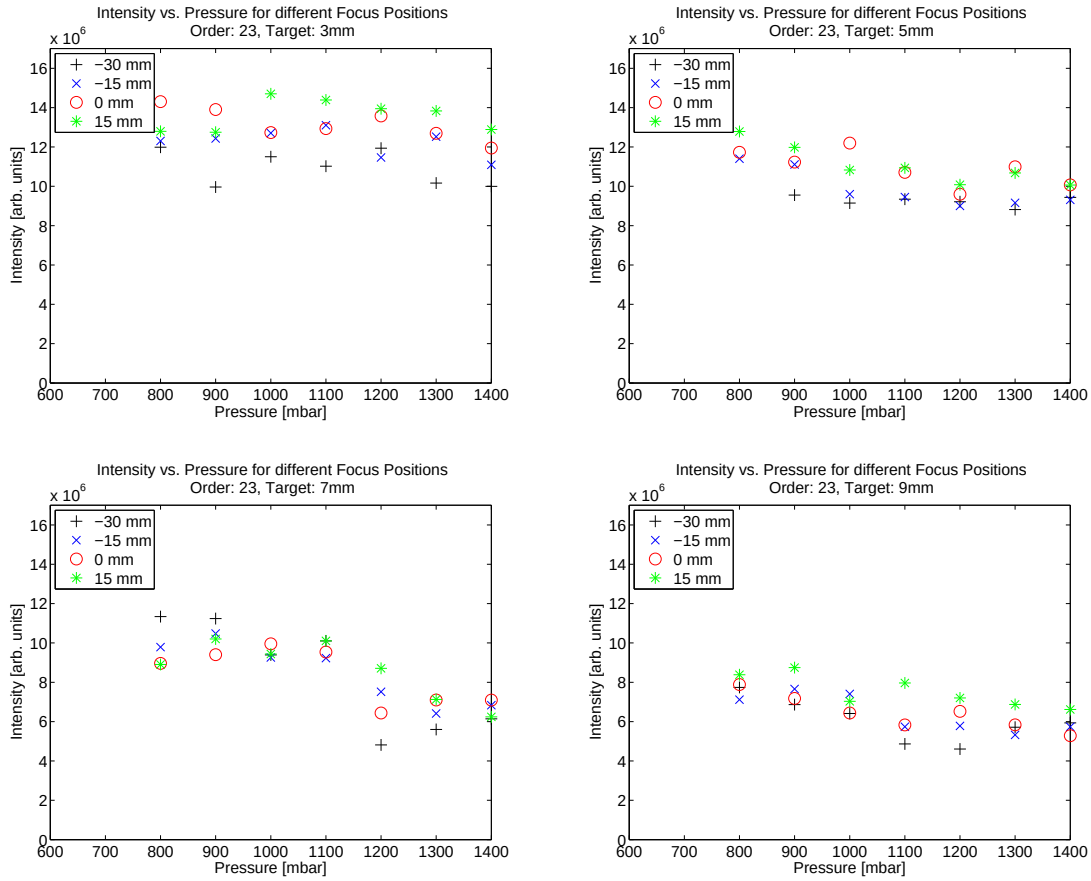

Figure 5.1: Intensity vs. pressure for 3 to 9 mm medium length for different focus positions. The intensity is almost constant or slightly decreasing with pressure and increases from −30 to 15 mm focus position.

intensities increase from −30 to 15 mm, especially for the shorter targets and the nozzle.

5.3 Pulse Energy and Aperture Dependence

We varied the pulse energy of the incident laser pulse by aperturing the beam by an iris. The pulse energy was measured by a power meter just after this iris but in front of the entrance window to the vacuum. The pulse energy is reduced by the entrance window by approximately 4%. All measurements were done with a background pressure of 1200 mbar and a focus position of 15 mm.

Figure 5.3 shows the results for harmonic order 23. After raising the pulse energy above a threshold of about 5 mJ the intensity of the harmonic increases rapidly with energy until it reaches its maximum. Increasing the pulse energy further leads to too high ionisation of the gas which affects phase matching conditions and results in lower intensities. This effect is the same for all four target lengths and the nozzle.

Comparing the position of the maximum of the curves of the four different cell lengths

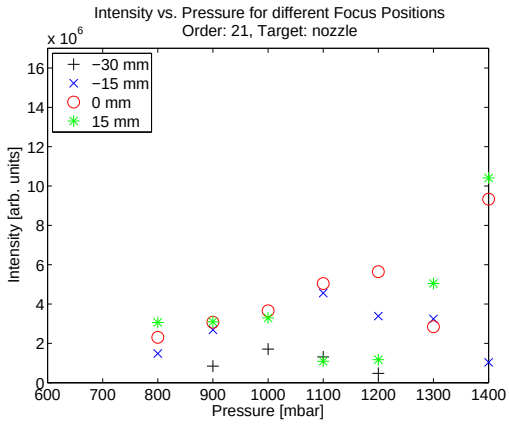

Figure 5.2: Intensity vs. pressure for a nozzle. The intensity of the generated harmonic increases with pressure.

we see that it is located at a higher pulse energy the longer the cell. This behaviour is shown by all harmonic orders.

For pulse energies lower than approximately 10 mJ the intensity of the harmonic is larger for shorter lengths of the cell. For larger energies this turns into the opposite: The intensity is larger for longer medium lengths than for shorter ones except for the 7 mm target where the intensities are lower than for the 5 mm target.

5.4 Comparison of the Intensity of one Harmonic between Cell and Nozzle

The most important question of our project was how much intensity increases when using a cell instead of a nozzle. We discuss this question in this section.

Looking at Figure 5.3 and taking the maximum of both the 23rd harmonic generated by the 9 mm target and the one generated by the nozzle we get a ratio of approximately $2.2 : 0.5 = 4.4 : 1$. It might be that this ratio changes slightly if we use higher pressure because as we have seen before the intensity increases with pressure for the nozzle but stays mostly constant for the cell. Therefore we estimate that the gain we get using the cell instead of the nozzle is about 4 times.

5.5 Spatial Distribution

In the following we analyse the impact of focus position and target length on the profile of the harmonics. The three dimensional plots show the intensity (colour) as a function of λ (vertical) and θ (horizontal).

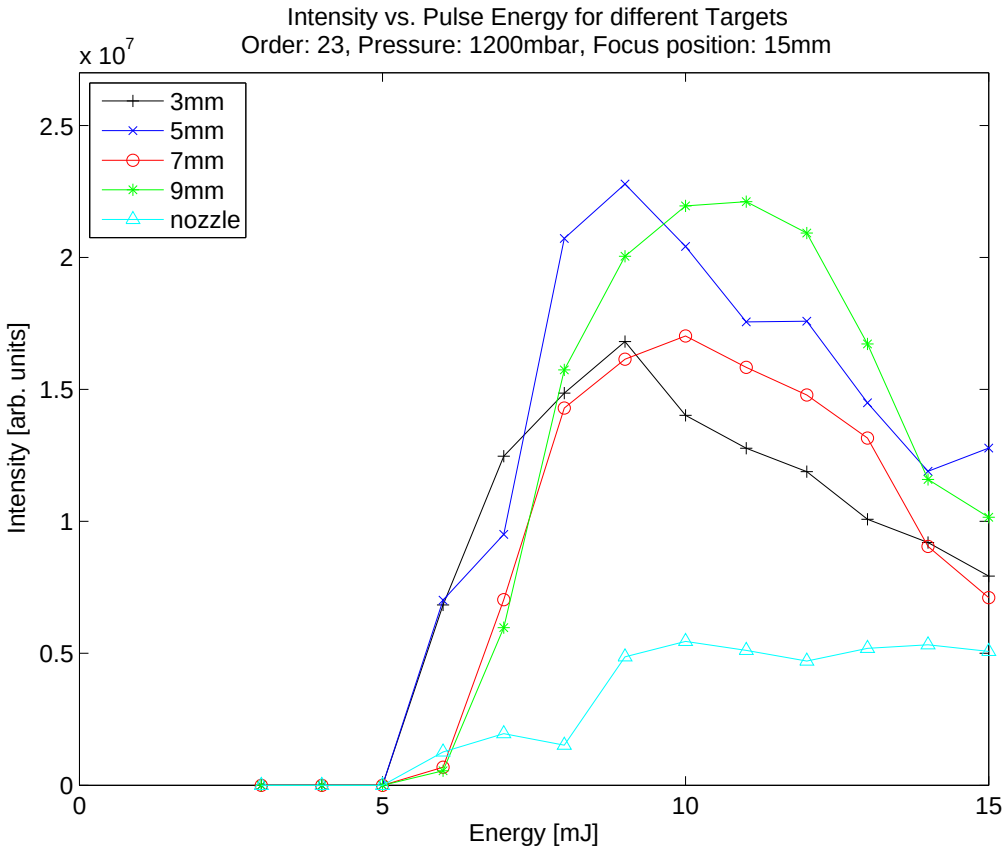

Figure 5.3: Intensity vs. pulse energy for different targets. After reaching a energy threshold the intensity of the harmonic increases rapidly until it gets saturated. Saturation and the slow decrease of the curves are due to higher ionisation ratios that effect phase matching.

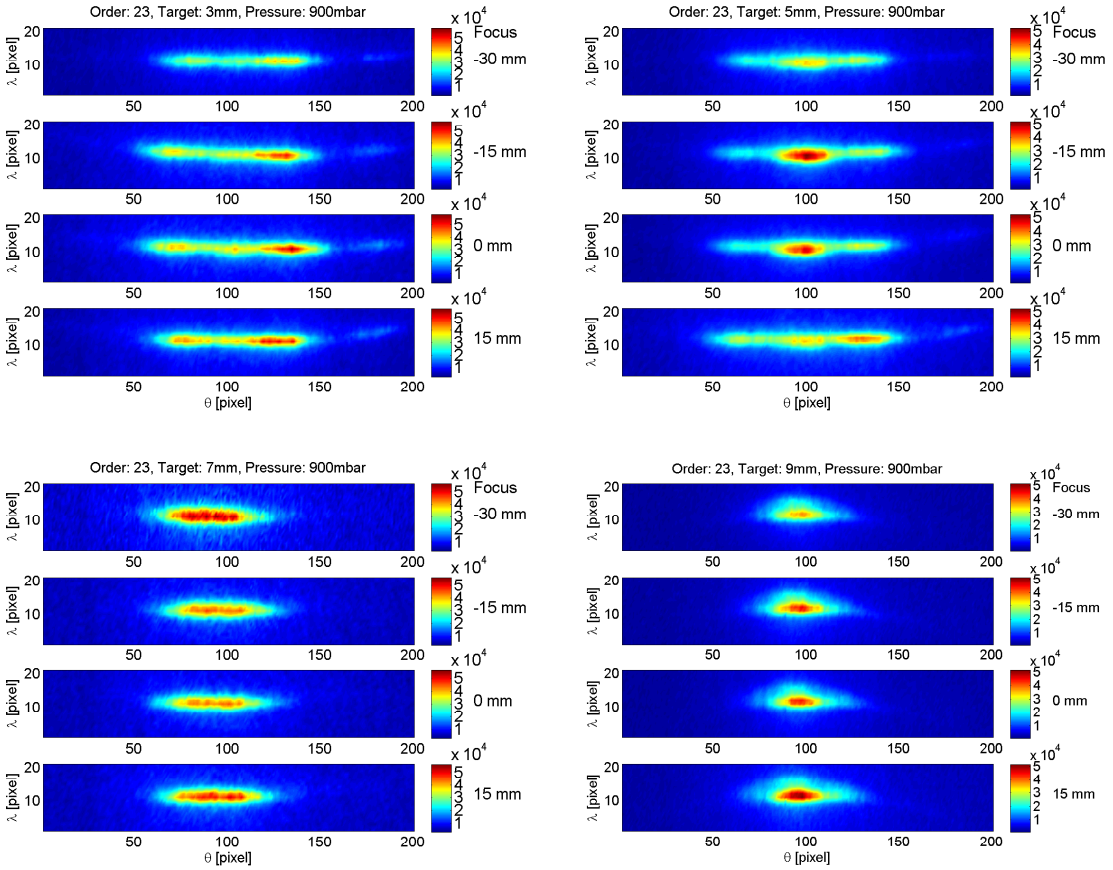

Figure 5.4: Intensity (colour) as a function of λ and θ for medium lengths of 3 to 9 mm. The profile of the harmonic does not change significantly with focus position.

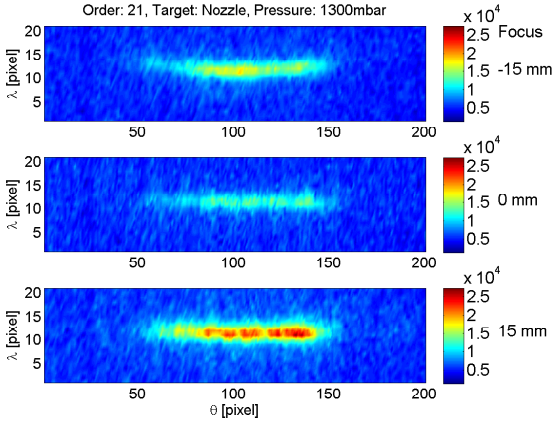

Figure 5.5: Intensity (colour) as a function of λ and θ for the 21st harmonic generated by the nozzle. The profile of the harmonic does not change much with focus position.

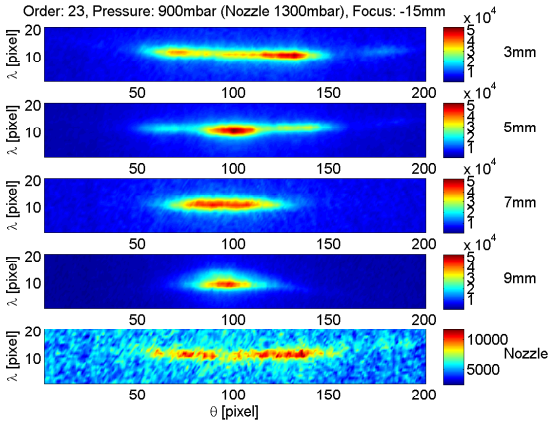

Figure 5.6: Intensity (colour) vs. λ and θ for different targets. We see a shift from the long trajectory at the 3 mm target to the short one at the 9 mm target. The nozzle plot shows a long trajectory harmonic.

5.5.1 Focus Position Dependence

Figure 5.4 shows the 23rd harmonic for different focus positions for target lengths of 3 to 9 mm. The pulse energy is 7 mJ, the aperture diameter 8 mm and the background pressure 900 mbar. All four plots show the same dependence of the focus position: The harmonic' profile does not change much in λ and θ. The profile of the harmonics change however with the target length, which is explored in more detail below. Figure 5.5 shows the same series with the nozzle for harmonic order 21. For -30 mm the harmonic is too weak to be clearly distinguished from the background and therefore omitted. For the other three focus positions the profile of the harmonics does not change very much.

5.5.2 Target Length Dependence

Figure 5.6 shows the target length dependence of the harmonic' profile of the 23rd harmonic for a pulse energy of 7 mJ, an iris diameter of 8 mm and a focus position of -15 mm. For the 3 to 9 mm targets the background pressure is 900 mbar and for the nozzle 1300 mbar.

For the 3 mm target we see the long trajectory, the short one is not visible. The 5 and 7 mm targets show both the short and the long trajectory and the 9 mm target shows mainly the short trajectory, the long one is very weak. The plot of the harmonic generated by the nozzle shows a long trajectory harmonic.

Chapter 6

Discussion

In Section 5.2 we have studied the pressure dependence of the harmonic' intensity. The pressure is related to the atom density N in the interaction region which has an impact on phase matching and therefore an impact on the intensity of the harmonics. The expected pressure dependence is that the intensity increases quadratically with pressure until a certain value is reached where it gets saturated. Our data seem to be in the saturated region for the cells but not for the nozzle. This might be both due to a shorter target length of only about approximately 0.5 mm when using the nozzle, and due to a lower atom density in the interaction region with the laser below the nozzle than we have in the cell.

The energy and aperture dependence was studied in Section 5.3. The target length dependence of the maximum of the intensity can be explained by the energy loss in regions in the medium with lower laser intensity because of the defocusing of the beam. The longer the medium the more energy is lost. By increasing the pulse energy this can be compensated. The decreasing intensity with increasing target length described in Section 5.2 can be explained with the intensity vs. pulse energy plot shown in Fig. 5.3, where at 7 mJ exactly this behaviour can be seen.

The focus position dependence studied in Section 5.5.1 is rather remarkable. We discovered that the profile of the harmonic in λ-θ space does not depend on the focus position. We did not observe double peaks and a shift from one peak to the other by changing the focus position, like Schütte did in [5]. He also found that the double peak structure depends on the compressor setting which corresponds to the chirp of the incident laser beam. It might be that our compression setting was set to such a value that the double peak structure is not observed. To find out if this is true or if there is really no double peak structure it will be necessary to observe the harmonics generated by the cell targets while changing the chirp.

The target length dependence was described in Section 5.5.2. As we have seen in Section 2.3 we can express the phase of the electric field of the harmonic in terms of $\alpha I(r,t)$. The long and the short trajectory add both to the electric field of the harmonic, so we can write:

$$E = E_L e^{-i\alpha_L I(r,t)} + E_S e^{-i\alpha_S I(r,t)},$$

where the long trajectory part is indexed by L and the short one indexed by S. Because

α_L and α_S are different the one or the other might be selected by phase matching. In our case it seems that the long trajectory is selected by short and the short trajectory by long targets.

Chapter 7

Conclusion and Outlook

We succeeded in improving the experimental setup by adding a way of aligning the beam without releasing the vacuum in form of a camera system which allows us to look at the entrance slit of the spectrometer and the reflection of the laser beam hitting it. We have also succeeded in building a new gas target which length can be varied by adding small plates. We studied its characteristics by measuring the pressure, focus position and energy and aperture dependence of the intensity of harmonics generated with Argon. Furthermore we have studied the focus and target length dependence of their λ-θ profile.

We found out that the harmonics' profile does not depend on the focus position and we did not observe a double peak structure. Instead of that we probably observed a shift from the long to the short trajectory with increasing medium length. We also found out that the intensity of harmonics is higher for a focus behind the middle of the medium than at or in front of and that the intensity is higher for larger medium lengths. Comparing the intensity of one harmonic order generated by the cell and the nozzle the intensity of the harmonic generated by the cell is about 4 times larger than the one generated by the nozzle.

Further research is needed in studying double peaks, e.g. to change the chirp of the driving laser field using the cell to generate harmonics instead of the nozzle in order to find out if not our compression setting was the reason why we have not observed them. Another possible measurement would be to cut the harmonics with the spectrometer's entrance slit to observe if they could be a result of misalignment. To further increase harmonics' intensity a looser focusing or a very long target, e.g. a long capillary with small diameter, could be considered.

Bibliography

[1] A. L'Huillier, Atoms in strong laser fields, Laboratory exercice, Advanced Atomic Physics

[2] L. Roos, Optimisation and Application of Intense High-Order Harmonic Pulses, Lund Reports on Atomic Physics, LRAP-276, Lund University, August 2001

[3] E. Mengotti, G. Genoud, Towards Time-Resolved X-UV Digital in-line Holography, Lund Reports on Atomic Physics, LRAP-368, Lund University, September 2006

[4] S. Häßler, M. Swoboda, Optimization and Application of High-order Harmonics of an Ultrashort Terawatt Laser, Lund Reports on Atomic Physics, LRAP-324, Lund University, June 2004

[5] B. Schütte, Optimization of High-order Harmonic Generation using an Ultrashort Pulse High-Intensity Laser, Lund Reports on Atomic Physics, LRAP-360, Lund University, May 2006

Appendix A

Documentation

This section should be understood as a manual how the setup can be used to create harmonics and how to acquire data. Maybe it will give some helpful hints even if the setup is changed.

A.1 Short description of the setup

A sketch of the setup is shown in Figure A.1.

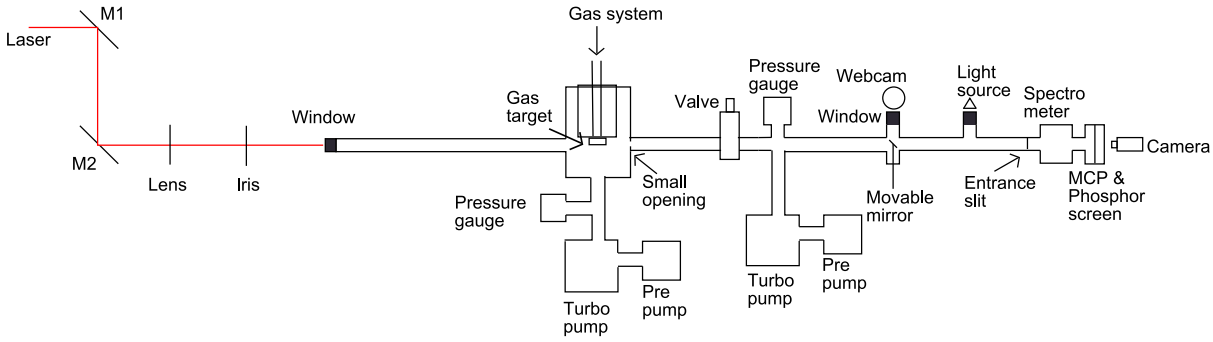

Figure A.1: Setup for high-order harmonics generation

In principle the setup works as follows: The lens focusses the beam on the gas target. Due to the interaction of the laser pulses with the argon gas, high order harmonics are generated. The spectrometer is used to observe different harmonics. The radiation is made visible using a multi channel plate with a phosphor screen and observed with a camera.

A.2 Alignment

For the Alignment it is better to use a low intensity laser beam. The lens position should be chosen so that the focus is at the middle of the gas target. This is approximately the 55 cm position on the translation stage. Be careful that the focus does not move

perpendicular to the beam direction when the lens position is changed. This can happen if the lens is not fixed correctly at the translation stage.

Mirrors M1 and M2 are used to align the beam. The first time the alignment is performed without vacuum. The MCP should not be mounted at this time since it has to stay under vacuum. Repeat the following steps:

- Use mirror M1 to align the beam at the gas-target.
- Use mirror M2 to align the beam on the entrance slit and control it using florescent yellow paper.

When the alignment is complete, the iris can be placed in a position so that it equally cuts the beam on every side when it is closed. The purpose of the iris is to reduce the beam power and to simplify the alignment.

The position of the spectrometer can also be slightly changed. A good position is found when you can see 'arcs' at the exit slit using a yellow paper. The spectrometer can also be opened to check if the beam hits the grating correctly. Doing this it is important not to touch the grating since it will be destroyed!

The alignment can now be performed while the system is under vacuum:

- Use mirror M1 to align the beam on the iris.
- Use mirror M2 to align the beam at the entrance slit of the spectrometer. This can be controlled using the webcam and the movable mirror.

A.3 The vacuum system and the gas system

The vacuum system can be divided into two parts using the valve (see Figure A.1). Both parts are pumped by a turbo molecular pump connected with a pre-pump. The pressure should be $< 10^{-5}$ mbar for harmonics generation and especially not to damage the MCP.

The gas system allows to set a constant background pressure for the argon gas. A reasonable value is around 1000 mbar.

A.4 Mounting of the gas target

Figure A.2 shows the part where the old target can be tightened.

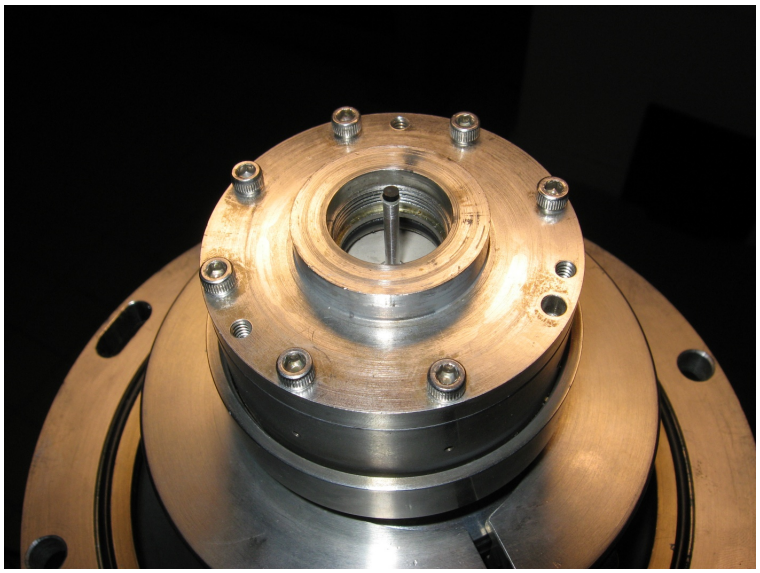

Figure A.2: Here the old gas target can be screwed in. The stamp in the middle is connected to the piezo-membranes

One can see the stamp that is connected to the piezo crystal and that moves in order to release the gas. To mount the target, you have to remove the outer ring, see Figure A.3.

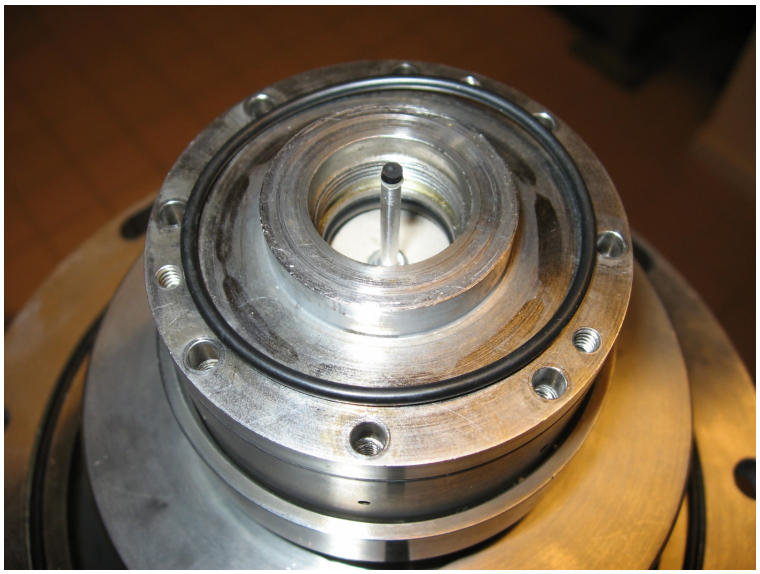

Figure A.3: The outer ring was removed. The O-Ring is necessary to have the next part in the right height.

The O-Ring is now used to have the target in the right height. The piece that is used as connection with the gas target is shown in the middle of Figure A.4.

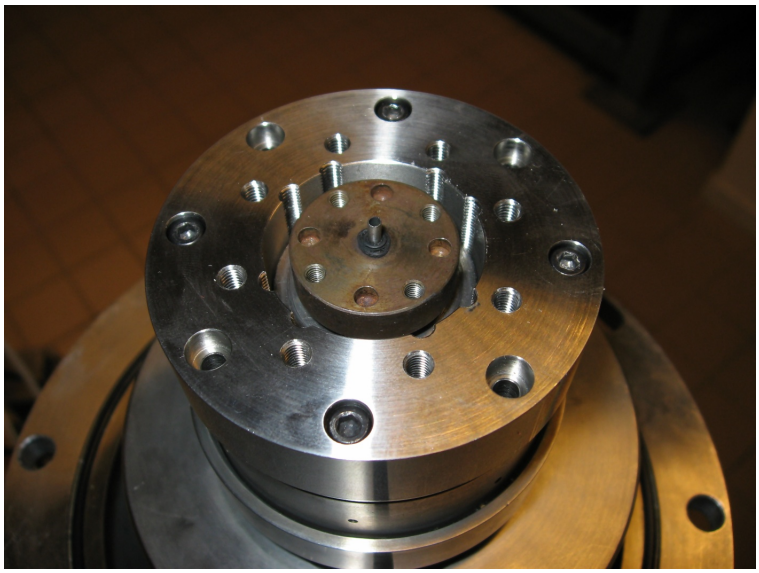

Figure A.4: The connection piece for the gas target and the outer ring was mounted.

In order to find the right position for it you should tighten it while you have a small gas background pressure. Stop tightening when almost no gas is leaking out. If you tighten it until there is no gas at all leaking out, you won't have any gas coming out of the target when it is mounted since it will push the connection piece down a bit.

Mount the outer ring and tighten the screws until it is at the same height as the middle part (therefore the O-Ring). Now you can mount the actual target, see Figure A.5.

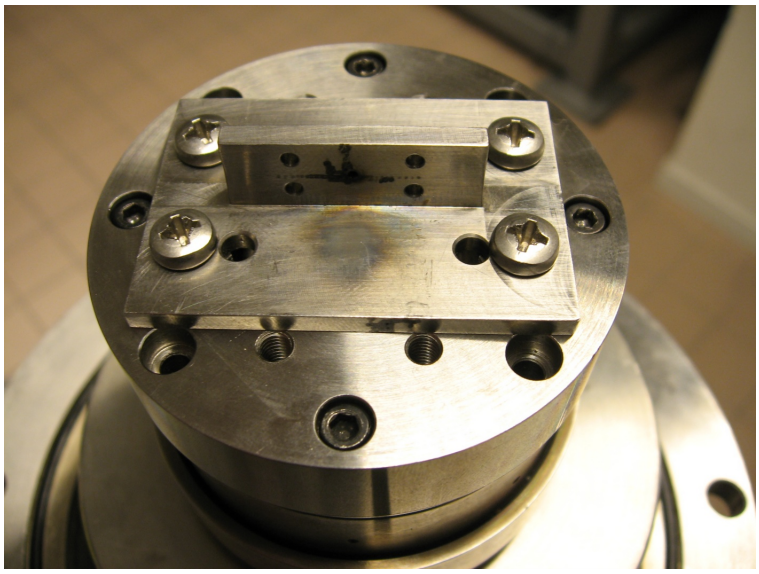

Figure A.5: The gas target is mounted and can be used.

Check if you can feel the gas streaming out of the target on both sides. If this is not the case you have to remove the last part again and loose the connection piece a little bit. This procedure can take a while.

A.5 Using the MCP

A sketch how the MCP and the phosphor-screen should be connected is shown in Figure A.6.

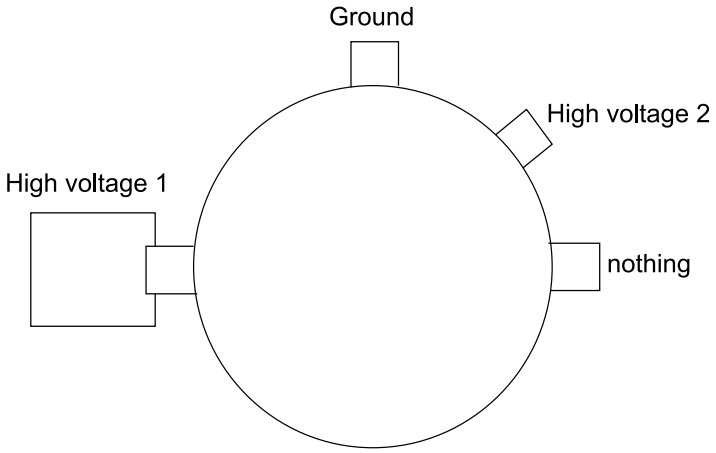

Figure A.6: Connecting the MCP and the phosphor screen

It is important that the pressure is $< 10^{-5}$ mbar before the high voltage is applied. Two high voltage sources are used, denoted as 1 and 2. The small displays at the high voltage generators show the voltage that will be applied, the big displays the actual voltage. Pressing `Enter` applies the voltage. (The `High voltage` button has to be turned on) The voltage should be increased slowly. It might be done as follows:

- Set 1 in steps of 100 V to +1000 V
- Set 2 in steps of 100 V to −1000 V
- Set 1 in steps of 100 V to +3000 V
- Set 2 in steps of 100 V to −1600 V

The maximum voltages that can be used are +3000 V and −2000 V respectively. High voltage 2 can be varied to change the brightness of the image.

A.6 Taking data

In order to watch different harmonics the grating in the spectrometer can be varied. It must not be turned to the 0 position while the laser beam is turned on! To obtain good images the camera has to be synchronized with the laser pulses. Therefore the trigger-connector must be connected with the `Trig out` port of pulsed valve driver box used in the gas system.

The program to acquire data is called `VMI\_Acq\_Dbg.exe` in the folder `c:\Marlin\_Acq`. A screenshot is shown in Figure A.7.

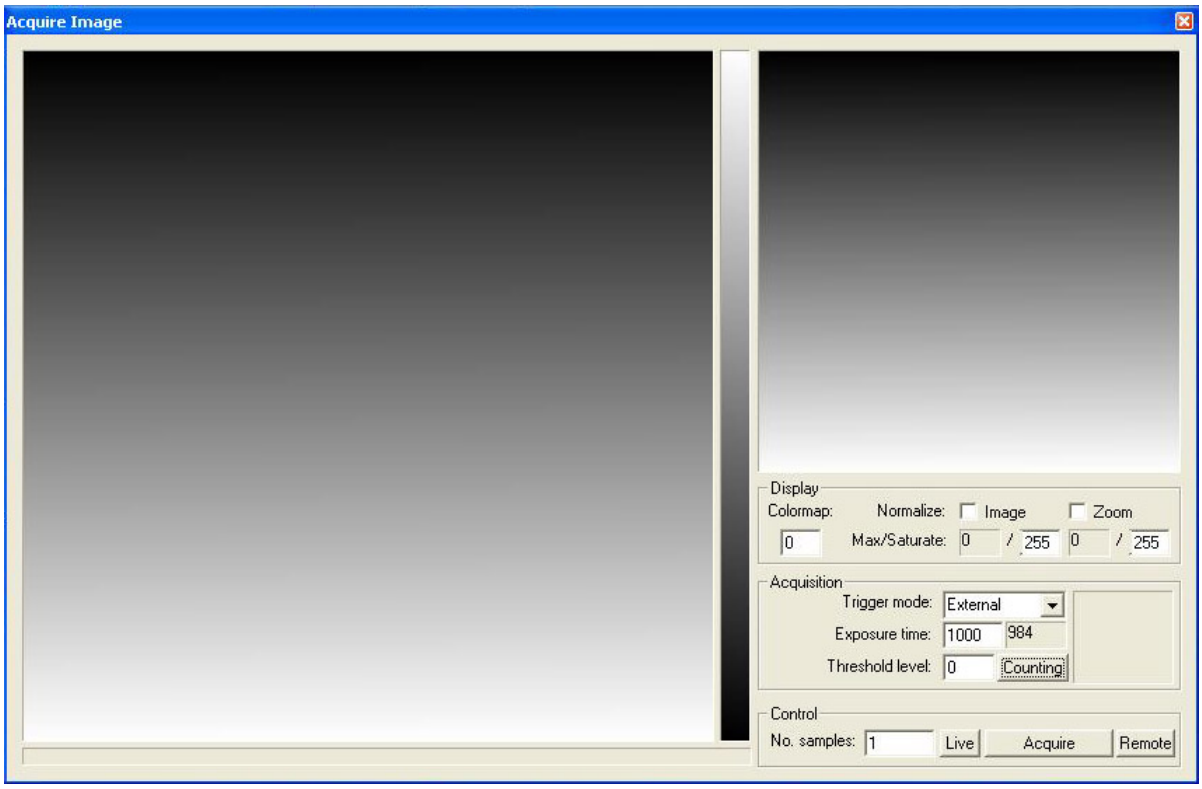

Figure A.7: Screenshot of the program used for taking images

The following settings can be used:

- Trigger mode: `external`
- Exposure time: 40000
- No. Samples: 40

To start a measurement press `Remote`, then `Acquire`. Be sure that the image is not saturated! If it is saturated, the high voltage 2 should be decreased. The image is then saved in `c:\temp\file.txt`. To convert it to a `tiff` file, the program `ImageJ` is needed:

- Go to `Plugins` → `Edit`
- Change to the macros folder
- Open file: `openSpectrum.txt`
- Set `filename="[yourFilename]"`
- Set `dir2="[outputPath]"`
- Choose `Macros` → `Install Macros`
- Choose `File` → `Run Macro`

A.7 Possible improvements

It would be a good idea to change the position of the lens with the position of the iris since in our case the beam is already slightly focussed when it passes the iris.

Another point would be to introduce an Aluminium-Filter somewhere behind the gas-target. It has the purpose to filter out the incident laser beam and let through only the harmonics.

Appendix B

Construction sketches for the gas target

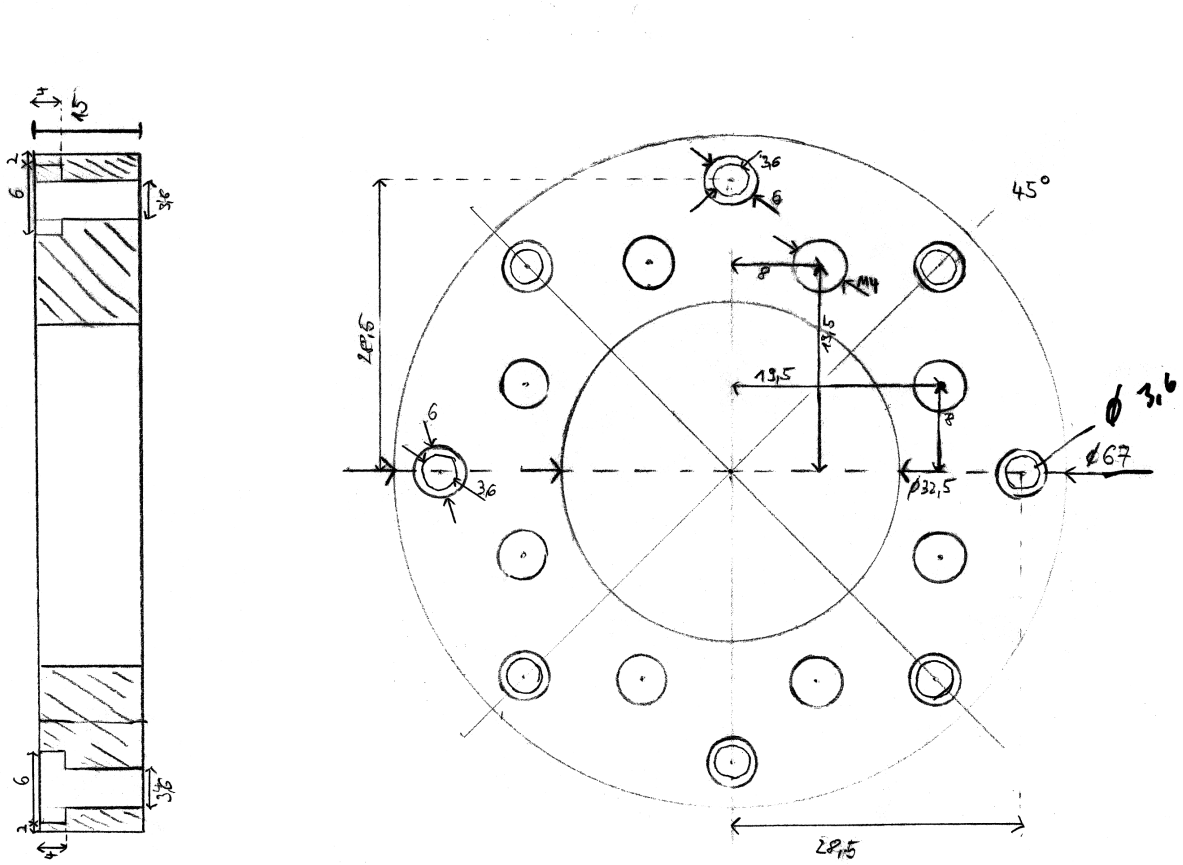

Figure B.1: Outer ring where the target is mounted on.

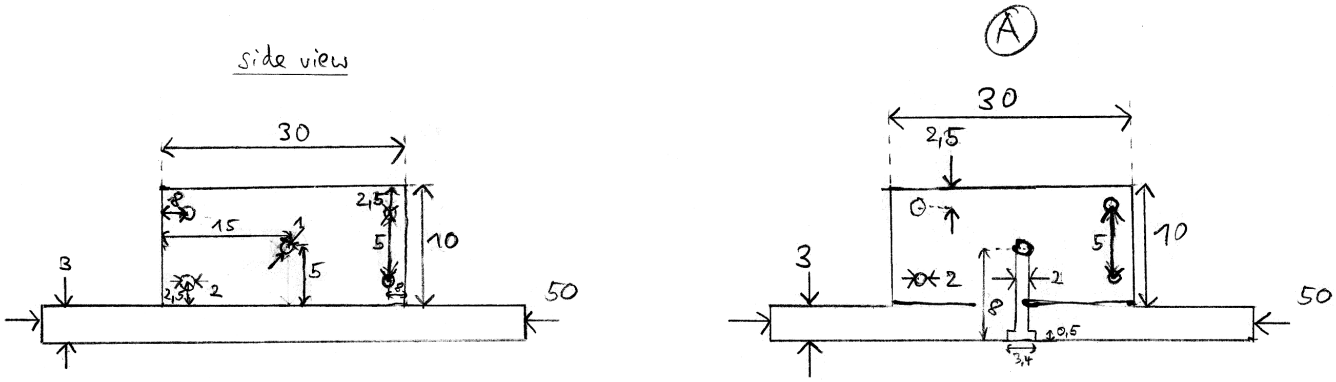

Figure B.2: The actual target, sideview

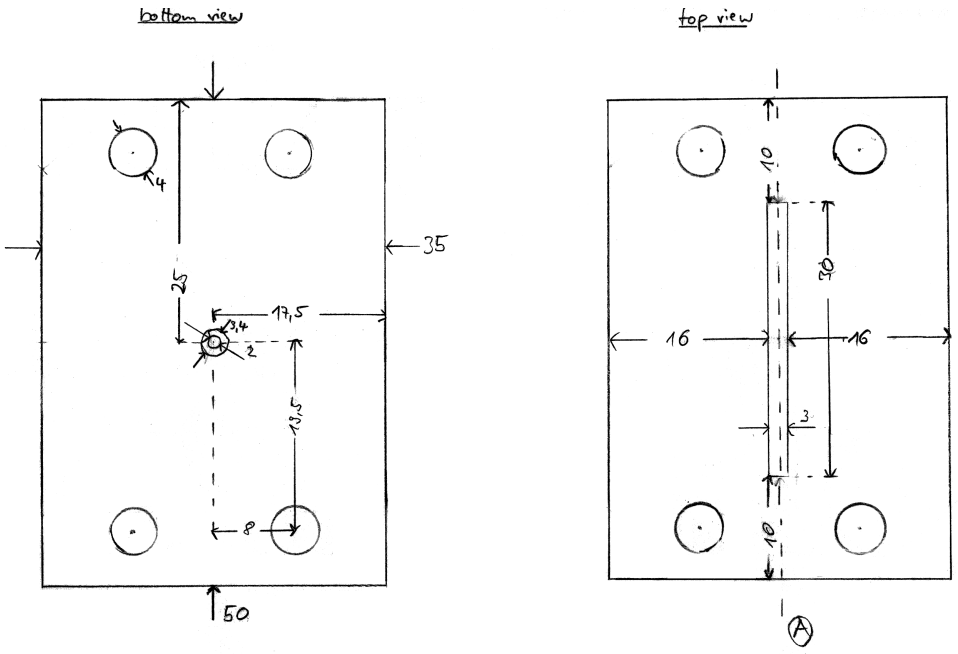

Figure B.3: The actual target, top and bottom view

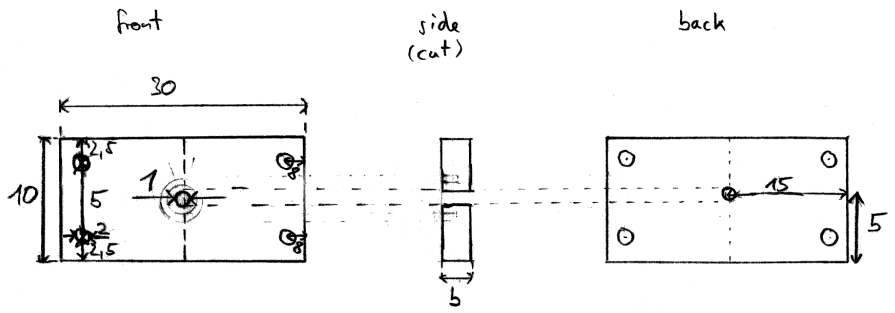

Figure B.4: Plate used for the elongation of the target.

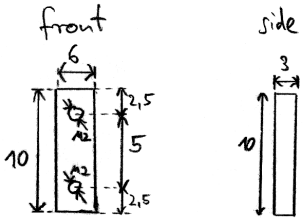

Figure B.5: Ending piece for the screws.